### Supplemental Table 1: Blood counts, BALF analyses and ricin catalysis products in CD-1 mice following application of low-dose ricin

| | | **sham mice** | **LDR mice-day 0**<br>(*p* value *vs*. sham) | **LDR mice-day 7**<br>(*p* value *vs*. sham) |
|---|---|---|---|---|
| **complete blood count[A]** | WBC (K/μl) | 4.51±1.68 | 10.64±1.78 (**0.003**) | 6.04±4.72 (0.564) |
| | NEU (K/μl) | 0.58± 0.92 | 1.82±4.81 (**0.007**) | 1.39±1.18 (0.496) |
| | MO (K/μl) | 0.17±0.17 | 0.73±0.22 (**0.007**) | 0.14±0.14 (0.809) |
| | PLT (K/μl) | 499±220 | 942±197 (**0.024**) | 734±217 (0.205) |
| **bronchoalveolar lavage fluid[B]** | protein (mg/ml) | 1.56±0.21 | 2.01±0.18 (**0.006**) | 4.44±1.7 (**0.007**) |
| | cholinesterase (mOD/min) | <5 | 355±143 (**0.0001**) | <5 |
| | cells (x$10^6$) | 36±27 | 86±27 (**0.019**) | 17.2±7.6 (0.178) |
| | IL-6 (pg/ml) | 34±29 | 586±110 (**4.47E-06**) | 75±30 (0.06) |
| | IL-1β (pg/ml) | 1±2 | 28±15 (**0.004**) | 43±41 (0.052) |
| | TNF-α (ng/ml) | 8±12 | 38±12 (**0.005**) | 28±22 (0.109) |
| **ricin catalysis products in lungs[B]** | depurinated 28S rRNA (%) | 0.22±0.31 | 7.94±3.11 (**0.00056**) | 0.42±0.6 (0.53) |

[A] n=4; [B] n=5. Statistically significant *t*-test values ($p<0.05$) are presented in bold type.

## Supplemental Table 2: Significant upregulated GO terms*

### Biological Process:

| GO ACCESSION | GO TERM | FDR | # of DEGs |
|---|---|---|---|
| GO:0050911 | detection of chemical stimulus involved in sensory perception of smell | 1.49E-29 | 7 |
| GO:0070098 | chemokine-mediated signaling pathway | 2.70E-16 | 33 |
| GO:0035458 | cellular response to interferon-beta | 3.03E-12 | 17 |
| GO:0010469 | regulation of signaling receptor activity | 1.41E-11 | 99 |
| GO:0051092 | positive regulation of NF-kappaB transcription factor activity | 5.39E-11 | 35 |
| GO:0045071 | negative regulation of viral genome replication | 1.94E-10 | 21 |
| GO:0032755 | positive regulation of interleukin-6 production | 4.51E-10 | 27 |
| GO:0042832 | defense response to protozoan | 7.56E-10 | 17 |
| GO:0010575 | positive regulation of vascular endothelial growth factor production | 1.05E-09 | 14 |
| GO:0006270 | DNA replication initiation | 4.35E-09 | 16 |
| GO:0032729 | positive regulation of interferon-gamma production | 7.02E-09 | 25 |
| GO:0050830 | defense response to Gram-positive bacterium | 9.95E-09 | 28 |
| GO:0043123 | positive regulation of I-kappaB kinase/NF-kappaB signaling | 7.80E-08 | 34 |
| GO:0032735 | positive regulation of interleukin-12 production | 2.86E-07 | 14 |
| GO:0000028 | ribosomal small subunit assembly | 6.65E-07 | 10 |
| GO:0000281 | mitotic cytokinesis | 8.91E-07 | 17 |
| GO:1990830 | cellular response to leukemia inhibitory factor | 1.51E-06 | 32 |
| GO:0001916 | positive regulation of T cell mediated cytotoxicity | 1.94E-06 | 10 |
| GO:0032715 | negative regulation of interleukin-6 production | 2.23E-06 | 16 |
| GO:0048535 | lymph node development | 2.71E-06 | 13 |
| GO:1904874 | positive regulation of telomerase RNA localization to Cajal body | 4.33E-06 | 9 |
| GO:0032689 | negative regulation of interferon-gamma production | 5.66E-06 | 14 |
| GO:0000463 | maturation of LSU-rRNA from tricistronic rRNA transcript (SSU-rRNA, 5.8S rRNA, LSU-rRNA) | 8.92E-06 | 8 |
| GO:0070431 | nucleotide-binding oligomerization domain containing 2 signaling pathway | 8.92E-06 | 8 |
| GO:0045651 | positive regulation of macrophage differentiation | 8.92E-06 | 8 |
| GO:0090023 | positive regulation of neutrophil chemotaxis | 9.49E-06 | 11 |
| GO:0048147 | negative regulation of fibroblast proliferation | 1.46E-05 | 13 |
| GO:1904871 | positive regulation of protein localization to Cajal body | 2.03E-05 | 6 |
| GO:0042531 | positive regulation of tyrosine phosphorylation of STAT protein | 2.67E-05 | 16 |
| GO:1903955 | positive regulation of protein targeting to mitochondrion | 3.46E-05 | 21 |
| GO:0032733 | positive regulation of interleukin-10 production | 3.75E-05 | 12 |
| GO:0032731 | positive regulation of interleukin-1 beta production | 3.75E-05 | 12 |
| GO:0045730 | respiratory burst | 5.79E-05 | 11 |
| GO:0032743 | positive regulation of interleukin-2 production | 6.06E-05 | 12 |
| GO:0043011 | myeloid dendritic cell differentiation | 6.07E-05 | 9 |
| GO:1901998 | toxin transport | 6.39E-05 | 15 |
| GO:0090026 | positive regulation of monocyte chemotaxis | 6.90E-05 | 8 |
| GO:0046641 | positive regulation of alpha-beta T cell proliferation | 8.54E-05 | 10 |
| GO:0051897 | positive regulation of protein kinase B signaling | 9.12E-05 | 21 |
| GO:0038094 | Fc-gamma receptor signaling pathway | 1.14E-04 | 6 |
| GO:0071359 | cellular response to dsRNA | 1.20E-04 | 9 |
| GO:0032211 | negative regulation of telomere maintenance via telomerase | 1.20E-04 | 9 |
| GO:1900017 | positive regulation of cytokine production involved in inflammatory response | 1.20E-04 | 9 |
| GO:0043547 | positive regulation of GTPase activity | 1.26E-04 | 57 |
| GO:0043124 | negative regulation of I-kappaB kinase/NF-kappaB signaling | 1.29E-04 | 13 |
| GO:0002925 | positive regulation of humoral immune response mediated by circulating immunoglobulin | 1.64E-04 | 5 |
| GO:0071224 | cellular response to peptidoglycan | 1.64E-04 | 5 |
| GO:2001268 | negative regulation of cysteine-type endopeptidase activity involved in apoptotic signaling pathway | 1.64E-04 | 5 |
| GO:0075525 | viral translational termination-reinitiation | 1.64E-04 | 5 |
| GO:0032728 | positive regulation of interferon-beta production | 2.18E-04 | 12 |

### Molecular Function:

| GO ACCESSION | GO TERM | FDR | # of DEGs |
|---|---|---|---|
| GO:0003735 | structural constituent of ribosome | 2.79E-59 | 97 |
| GO:0004984 | olfactory receptor activity | 1.49E-29 | 7 |
| GO:0005524 | ATP binding | 1.78E-27 | 266 |
| GO:0008009 | chemokine activity | 9.22E-16 | 25 |
| GO:0005525 | GTP binding | 7.81E-11 | 77 |
| GO:0003743 | translation initiation factor activity | 3.54E-10 | 23 |
| GO:0045296 | cadherin binding | 4.29E-10 | 59 |
| GO:0003924 | GTPase activity | 9.02E-10 | 60 |
| GO:0031625 | ubiquitin protein ligase binding | 2.08E-09 | 58 |
| GO:0008270 | zinc ion binding | 2.66E-09 | 115 |
| GO:0042803 | protein homodimerization activity | 5.68E-09 | 117 |
| GO:0004298 | threonine-type endopeptidase activity | 2.23E-08 | 13 |
| GO:0003697 | single-stranded DNA binding | 2.44E-08 | 27 |
| GO:0005164 | tumor necrosis factor receptor binding | 2.86E-07 | 14 |
| GO:0003725 | double-stranded RNA binding | 3.05E-07 | 23 |
| GO:0048027 | mRNA 5'-UTR binding | 1.94E-06 | 10 |
| GO:0046982 | protein heterodimerization activity | 2.86E-06 | 75 |
| GO:0017116 | single-stranded DNA helicase activity | 4.33E-06 | 9 |
| GO:0051059 | NF-kappaB binding | 4.62E-06 | 11 |
| GO:0005031 | tumor necrosis factor-activated receptor activity | 9.49E-06 | 11 |
| GO:0000978 | RNA polymerase II cis-regulatory region sequence-specific DNA binding | 1.18E-05 | 78 |
| GO:0001530 | lipopolysaccharide binding | 1.83E-05 | 11 |
| GO:0047485 | protein N-terminus binding | 1.93E-05 | 23 |
| GO:0036402 | proteasome-activating ATPase activity | 2.03E-05 | 6 |
| GO:0000049 | tRNA binding | 2.11E-05 | 15 |
| GO:0001054 | RNA polymerase I activity | 2.73E-05 | 8 |
| GO:0003730 | mRNA 3'-UTR binding | 5.80E-05 | 17 |
| GO:0001056 | RNA polymerase III activity | 6.07E-05 | 9 |
| GO:0003746 | translation elongation factor activity | 6.07E-05 | 9 |
| GO:0008017 | microtubule binding | 1.08E-04 | 46 |
| GO:0016176 | superoxide-generating NADPH oxidase activator activity | 1.14E-04 | 6 |
| GO:0001228 | DNA-binding transcription activator activity, RNA polymerase II-specific | 1.47E-04 | 65 |
| GO:1990825 | sequence-specific mRNA binding | 1.64E-04 | 5 |
| GO:0097677 | STAT family protein binding | 1.64E-04 | 5 |
| GO:0036002 | pre-mRNA binding | 2.46E-04 | 10 |
| GO:0051082 | unfolded protein binding | 3.35E-04 | 19 |
| GO:0043130 | ubiquitin binding | 4.05E-04 | 16 |
| GO:0003755 | peptidyl-prolyl cis-trans isomerase activity | 4.55E-04 | 12 |
| GO:0043022 | ribosome binding | 5.39E-04 | 14 |
| GO:0042056 | chemoattractant activity | 6.07E-04 | 10 |
| GO:0051117 | ATPase binding | 6.65E-04 | 16 |
| GO:0003724 | RNA helicase activity | 6.65E-04 | 16 |
| GO:0003713 | transcription coactivator activity | 7.32E-04 | 40 |
| GO:0061631 | ubiquitin conjugating enzyme activity | 7.77E-04 | 11 |
| GO:0010997 | anaphase-promoting complex binding | 7.77E-04 | 5 |
| GO:0043023 | ribosomal large subunit binding | 7.77E-04 | 5 |
| GO:0051539 | 4 iron, 4 sulfur cluster binding | 8.73E-04 | 12 |
| GO:0008137 | NADH dehydrogenase (ubiquinone) activity | 9.63E-04 | 8 |
| GO:0004550 | nucleoside diphosphate kinase activity | 9.63E-04 | 8 |
| GO:0003887 | DNA-directed DNA polymerase activity | 9.74E-04 | 9 |

***** Top 50 GO terms of biological processes and molecular function terms, with their false discovery rate (FDR) value and the number DEGs in lungs of LDR mice compared to naïve (n=4).

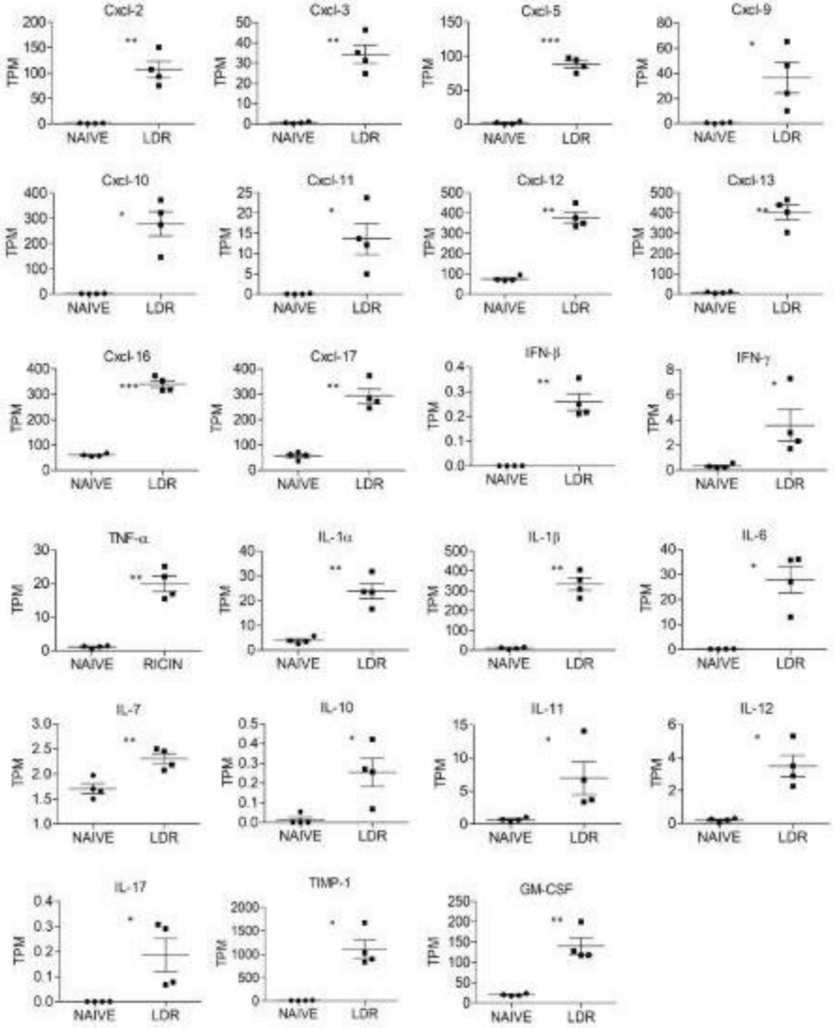

**Supplemental Figure 1: Effects of low dose ricin application on cytokine and chemokine gene expression in lungs of CD-1 mice**. Normalized gene expressed levels (transcripts per million, TPM) of 23 indicated cytokines and chemokines determined from RNAseq data of LDR mice (2 days post-low-dose-ricin-application) compared with naïve control. Data are represented as average ± SEM (n=4 per group) analyzed using unpaired t-test. **p* <0.05, ***p* <0.01, ****p* <0.001

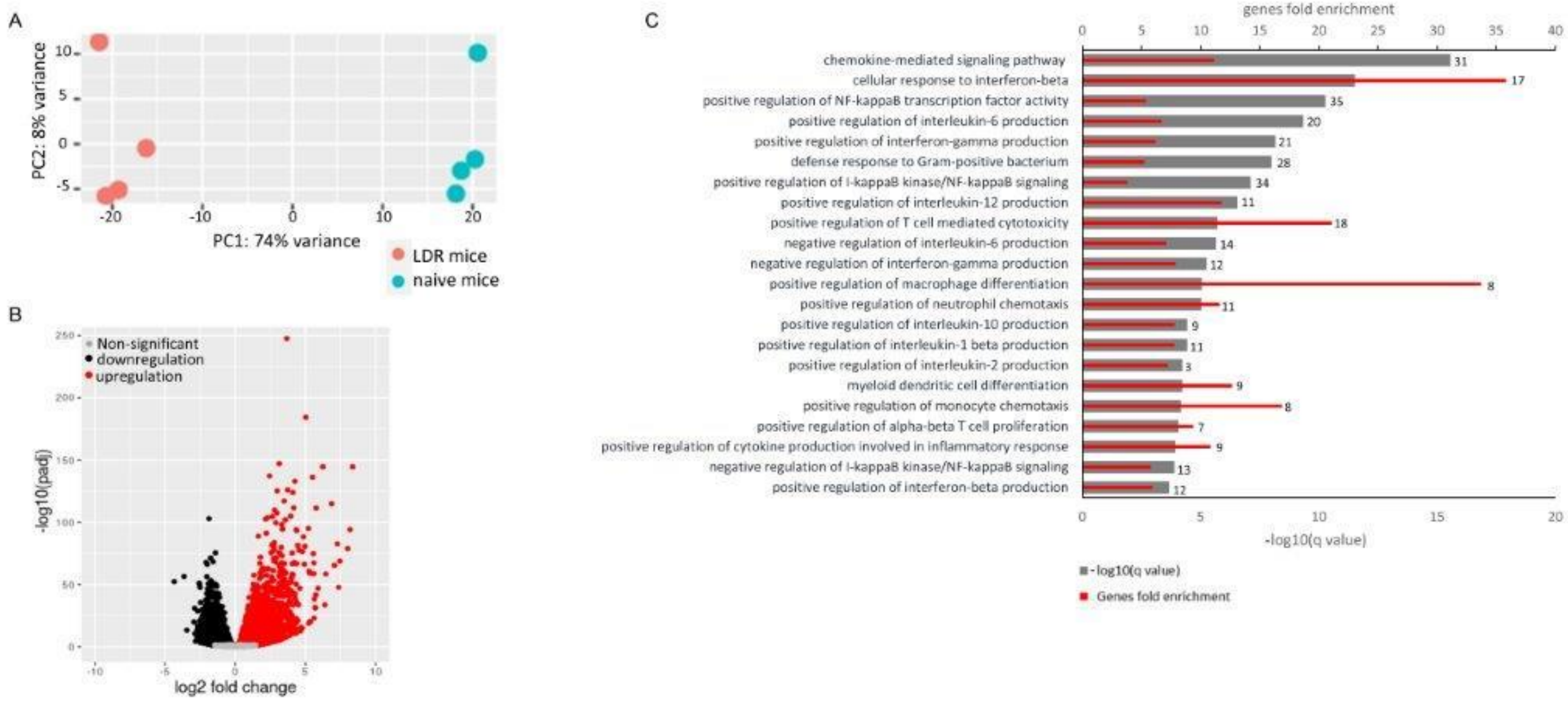

**Supplemental Figure 2: Distinct transcriptional signatures in LDR mice compared to naïve mice**. RNAseq analysis of lung homogenates from naïve- and LDR- (2 days post-low-dose-ricin application) mice (n=4). A: Principal component analysis was performed for 8 samples with log2 transformed gene-level normalized counts data. PC, principal component. B: Volcano plot comparing differentially expressed genes, respectively, with a false discovery rate (q value) < 0.05. Multiple comparisons were accounted for by calculation of a Benjamini-Hochberg false discovery rate-adjusted P value (q value). Each dot in the volcano plot represents a single gene. C: Gene Ontology (GO) enrichment analysis of biological process (BP) terms enriched in upregulated genes from comparisons of LDR mice versus naïve. Terms were ranked by the false discovery rate (q value) and the immune and inflammatory terms are listed from the top 50 after eliminating redundant terms. Gray bars show the –log10[q value]. Red bars show the genes fold enrichment.

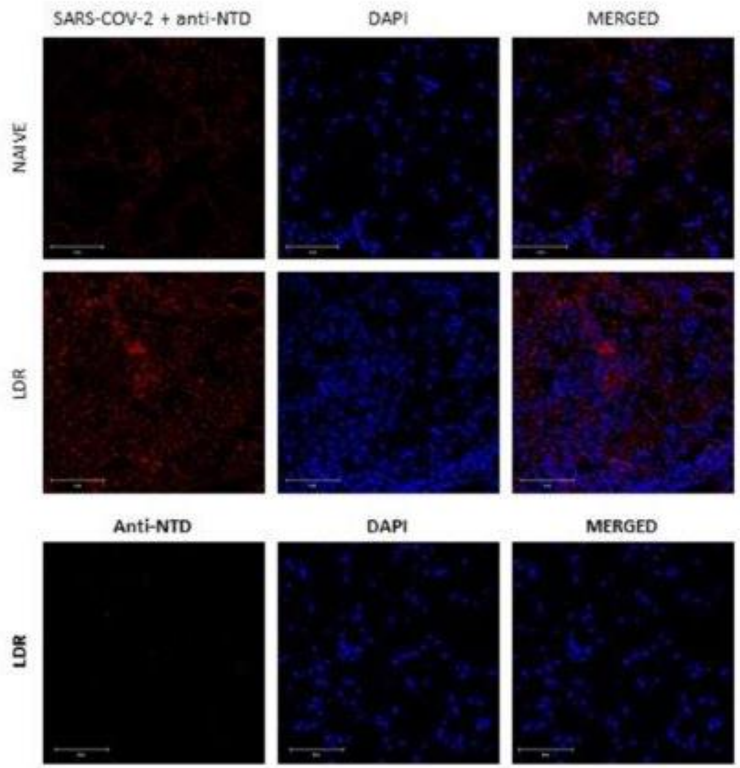

**Supplemental Figure 3: Confocal microscopy scans of lung sections.** Lung sections prepared from naïve (upper row) or LDR mice at 2 days post-ricin administration (middle row) were incubated with SARS-CoV-2 (1000 PFU/ml) and then immunostained with a monoclonal antibody directed against the spike region of the SARS-CoV-2, followed by AF594-labeled anti-human antibody. Lung sections of LSR mice incubated with vehicle only (no virus) served as a negative control for the anti-SARS-CoV-2 monoclonal antibody (bottom row). Staining of SARS-CoV-2 in red and identification of nuclei by DAPI in blue, bar= 50 µm. Representative sections of n=4 mice are shown.

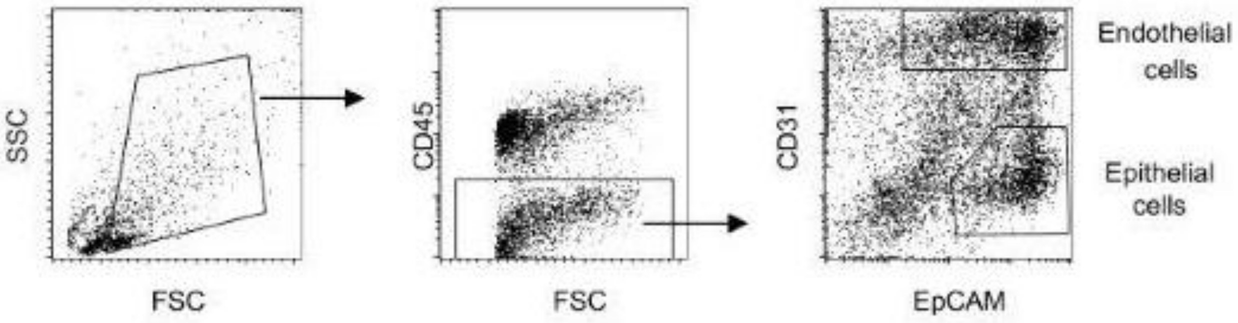

**Supplemental Figure 4: A hierarchical gating strategy to identify lung epithelial and endothelial cells.** Representative FACS plot (n=4) that identifies lung epithelial cells (CD45-CD31-EpCAM+) and endothelial cells (CD45-CD31+)